Medicine in Novel Technology and Devices 1 (2019) 100004

Contents lists available at ScienceDirect

Medicine in Novel Technology and Devices

journal homepage: www.journals.elsevier.com/medicine-in-novel-technology-and-devices/

Research Paper

Feature extraction based on empirical mode decomposition for automatic mass classification of mammogram images

Vaijayanthi Nagarajan [a,*], Elizabeth Caroline Britto [b], Senthilvel Murugan Veeraputhiran [c]

[a] Indra Ganesan College of Engineering, Department of Electronics and Communication Engineering, Manikandam, Tiruchirappalli, 620 012, India
[b] IFET College of Engineering, Department of Electronics and Communication Engineering, Valavanur, Villupuram, 605 108, India
[c] KAPV Government Medical College Hospital, Department of Radiology, Collector's Office Road, Tiruchirappalli, 620 001, India

ARTICLE INFO

Keywords:
Image processing
Image analysis
Image classification
Feature extraction
Mammography
Computer-aided diagnosis
Medical imaging
Empirical mode decomposition

ABSTRACT

Breast cancer is one of the major health problems that leads to early mortality in women. To aid the radiologists, computer aided diagnosis provides a second opinion for the detection and classification of breast cancer. In this paper, two texture feature extraction methods using Empirical Mode Decomposition (EMD) have been proposed to classify the masses in mammogram images into benign or malignant. The first feature extraction method is based on Bi-dimensional Empirical Mode Decomposition (BEMD). On performing BEMD on Region of Interest (ROI) of mammogram image, the ROI is decomposed into a set of different frequency components called Bi-dimensional Intrinsic Mode Functions (BIMFs). Gray Level Co-occurrence Matrix (GLCM) and Gray Level Run Length Matrix (GLRM) features are extracted from these BIMFs and are given as input to the classifier for classification into benign or malignant. Due to the mode mixing problem that exists in BEMD, BIMFs obtained from BEMD are less orthogonal to each other. To overcome this drawback, the second feature extraction method called Modified Bi-dimensional Empirical Mode Decomposition (MBEMD) is proposed. The BIMFs are extracted by employing the proposed MBEMD on mammogram ROI. Features are extracted in a similar way as BEMD method. Support Vector Machine (SVM) and Linear Discriminant Analysis (LDA) classifiers are used for the classification of mammogram mass. The classification accuracy of 88.8%, 96.2% and Area Under the Curve (AUC) of Receiver Operating Characteristics (ROC) of 0.9, 0.96 are obtained with SVM classifier for BEMD, proposed MBEMD based features respectively. The results show that the proposed method yields consistent performance when applied across different databases.

1. Introduction

Breast cancer is one of the major health problems that leads to early mortality in women, especially those between 40 and 55 years of age all over the world. In India, breast cancer accounts for 14% of all cancers in women and 1 in 28 women is likely to get affected by this disease during her lifetime [1]. According to global cancer report (GLOBOCAN 2018), 11.6% of new cases are the incidence of breast cancer with mortality rate of 6.6% of all cancer deaths that occurred world wide during 2018 [2].

Early detection of breast cancer in screening mammography is a challenging task because the appearances of breast cancer are unstable in the early stages. There are chances for the radiologists to misinterpret a normal region in the mammogram image as a suspicious lesion or to miss the abnormality in the image. To aid the radiologists in analyzing mammogram images, two automated systems have been developed: (i) Computer-Aided Detection system to detect and segment the lesions in mammograms. (ii) Computer-Aided Diagnosis (CADx) system to classify the detected lesions into benign or malignant [3]. The main objective of our research work is to develop an efficient feature extraction method to classify the masses in mammograms into benign or malignant.

In recent years, many feature extraction methods based on gray level, shape and texture features have been proposed for the classification of masses in mammogram images. Gray level features are first-order statistics such as mean, standard deviation and variance that are used to measure the intensity variation in mammogram images for discrimination between benign and malignant [4–6]. Feature extraction using shape features are based on the extraction of spatial arrangements of pixels such as area, perimeter, compactness and circularity to distinguish between mass and normal breast tissue [7–10]. Texture is an important characteristic for the classification of masses in mammogram images because it

* Corresponding author.
E-mail address: vaijuanand@hotmail.com (V. Nagarajan).

https://doi.org/10.1016/j.medntd.2019.100004
Received 21 June 2019; Received in revised form 25 August 2019; Accepted 8 September 2019

describes the spatial variation of pixel intensities in an image. It also determines smoothness or coarseness of image features. The techniques used for texture feature extraction from the image are structural, statistical and transform methods. The structural methods represent texture by well-defined primitives that provide a good symbolic description of the image [11,12]. The statistical approaches use the properties that govern the distribution and relationships of gray levels in the image. The most commonly used statistical methods are computed from GLCM and GLRLM [13–15]. The transform methods are based on the processing of the image in the transform domain. Texture features based on Gabor wavelets and Contourlet transform [12,16,17] are most widely used to extract texture features at different orientations.

After the features are extracted from the mammogram mass ROI, the classification of mass into benign or malignant is performed using classifiers. Among the classifiers, the most popular classifiers used by the researchers for mammogram mass classification are LDA, K-nearest neighbors, decision tree and SVM. Texture features based on Gabor filters was proposed by S. Khan et al. [12]. For classification SVM was implemented and an average accuracy of 93.95% was achieved. R. Rabidas et al. [11] proposed a texture feature extraction method based on neighborhood structural similarity. For classification, LDA was used and achieved an accuracy of 94.57%. In the method presented by X. Liu et al. [13], geometrical and textural features are incorporated with SVM classifier for mammogram mass classification. Accuracy of 94% was attained with this method. Ioan B et al. [16] extracted directional features using Gabor wavelets and proximal SVM was used to classify the data. A.K. Mohanty et al. [15] proposed a method for texture-based feature extraction and decision tree models were used for classification. The accuracy of 96.7% was achieved by this method. The performance of SVM and LDA is proved favorable for mass classification in the literature [12,13,16,17]. Hence, SVM and LDA classifiers have been implemented in this proposed feature extraction method for mammogram mass classification.

The main issues with the existing feature extraction methods are: (i) The methods that use gray level features achieved low accuracy in the classification of masses. (ii) Shape features are not sufficient enough to classify the mass into benign or malignant. It is only used to distinguish the mass region from normal breast tissue. (iii) Most of the texture feature extraction techniques are based on transform methods and are non-adaptive in nature because it uses filtering scheme or basis functions. The existing feature extraction methods resulted in a large feature set and hence dimensionality reduction of the feature set or feature selection must be performed which adds complexity to the diagnosis system.

The proposed method addresses the above problems by incorporating a multiresolution decomposition technique called BEMD for texture feature extraction. BEMD does not use any basis functions, hence differs from Fourier transform and wavelet transform. BEMD is a decomposition method which is used to decompose the image into a set of Bi-dimensional Intrinsic Mode Functions (BIMFs) or modes. BEMD has been used in texture analysis because the extracted BIMFs are the strong characteristics of the texture features. J.C Nunes et al. [18] has implemented BEMD for texture extraction and it was shown that none of the methods except BEMD performs best for all types of images for extracting texture features. BEMD has been employed for the classification of mammograms into normal and abnormal images [19]. Even though BEMD is a useful decomposition tool for texture analysis, it has the problem of mode mixing where a single IMF consists of signals of different scales or the mode will get mixed in another IMF.

To overcome the problem of mode mixing that exists in BEMD, a decomposition algorithm called MBEMD has been proposed in this method. The performance of BEMD and the proposed MBEMD is compared in terms of the Orthogonality Index (OI), Mean Square Error (MSE) and Peak Signal to Noise Ratio (PSNR). Both BEMD and the proposed MBEMD has been implemented in the proposed feature extraction method for classifying the masses into benign or malignant and the results are compared.

2. Materials and methods

The main objective of the proposed method is to classify the masses in mammograms into benign or malignant using two feature extraction methods: BEMD and the proposed MBEMD. Mammogram images for the proposed work have been collected from Mammographic Image Analysis Society (MIAS) Database, Digital Database for Screening Mammography (DDSM) which are the publicly available database. The images are also collected from the Department of Radiology, Mahatma Gandhi Memorial (MGM) Hospital, affiliated to KAPV Government Medical College, Tiruchirappalli, India. This local database is mentioned as MGM hospital images throughout this paper. The proposed work has been tested in MATLAB 8.0.0 environment on a computer with Intel Core i3 processor with 2.10 GHz CPU and 4 GB RAM.

MIAS database consists of 322 images of Medio Lateral-Oblique (MLO) view taken from 161 patients. The images were digitized to 200-μm pixel edge and resized to 1024 × 1024 [20]. Out of 322 images in MIAS database, 53 images with the benign type of masses and 39 images with malignant masses are taken for this work.

DDSM database consists of images taken from 2500 patients approximately. From every patient, two images, each from the left breast and right breast of both craniocaudal (CC) view and MLO view are taken. Out of these images, 60 images with benign masses and 60 images with malignant masses are taken for this work. Lumisys scanner at 50 mm pixel size and Howtek scanner at 43.5 mm pixel size are used to digitize the images that have been taken for this work. The pixel resolution of these images is 12 bits. The ground truth information about the abnormal areas in the images are given in the '.ics' file [21].

MGM hospital images consist of 176 images of both CC view and MLO view. The images are digitized to 100-μm pixel edge and the resulting digital images size are 1954 × 2410. Out of these images, 59 images with benign masses and 29 images with malignant masses are taken for this work. The block diagram of the proposed method is shown in Fig. 1. The proposed method feature extraction method consists of the following steps: (i) Pre-processing to enhance the image. (ii) ROI Extraction to crop the mass region. (iii) Decomposition of ROI based on BEMD and the proposed MBEMD into BIMFs or modes. (iv) Extraction of GLCM, GLRLM features from these BIMFs. (v) Classification of ROI into benign or malignant. For classification of ROI, SVM and LDA classifiers have been employed in this work. Finally, the results obtained by BEMD, MBEMD based feature extraction are compared in terms of accuracy and AUC of ROC.

2.1. Empirical mode decomposition (EMD) for feature extraction

EMD is a multiresolution decomposition technique that decomposes the signal into a set of different frequency components called Intrinsic Mode Functions (IMFs) and a residue. The decomposition method to obtain IMFs is called sifting process. EMD does not use any basis functions and it is suitable for non-linear, non-stationary data analysis, EMD can be considered as filtering technique [22].

2.1.1. Bi-dimensional empirical mode decomposition: an overview

The two-dimensional (2-D) extension of EMD is called BEMD which can be used for 2D signals or images. BEMD is a decomposition algorithm which is used to decompose the image into a set of BIMFs. The decomposition of an image into its BIMFs is called sifting process.

For a function to be an IMF, the following two constraints must be satisfied. (i) The number of zero-crossing local extrema (maxima and minima) must be equal or differ by one at most. (ii) The mean value of the envelope defined by the extrema must be zero. The sifting process [18] to decompose the image $f(m,n)$ into its BIMFs with m rows, n columns in the image, is explained as follows: To extract first IMF from the image, the envelope of local maxima and minima of the image $f(m,n)$ is determined and its mean $E_1(m,n)$ is obtained. The function $g_1(m,n)$ is given by:

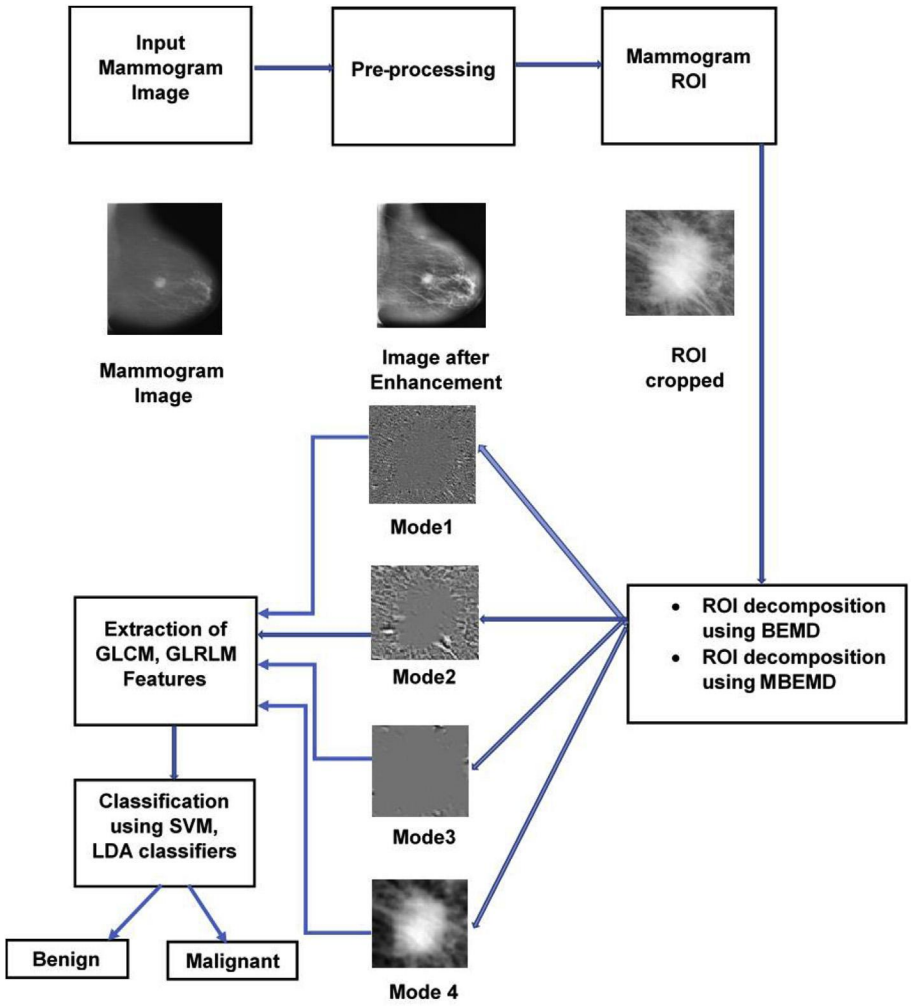

Fig. 1. Block diagram of the Proposed Feature Extraction method.

$$g_1(m,n) = f(m,n) - E_1(m,n) \tag{1}$$

If $g_1(m,n)$ satisfies the above said constraints of IMF, then it is designated as first IMF defined by $BIMF_1(m,n)$. If not, then it is considered as data and the sifting process is continued until an IMF is encountered. After determining first IMF, the first residue $R_1(m,n)$ is determined by:

$$R_1(m,n) = f(m,n) - BIMF_1(m,n) \tag{2}$$

The residue is considered as new data and the sifting process is continued until a new IMF $BIMF_2(m,n)$ is obtained. The second residue $R_2(m,n)$ can be determined by:

$$R_2(m,n) = R_1(m,n) - BIMF_2(m,n) \tag{3}$$

The subsequent residues are determined by:

$$R_k(m,n) = R_{k-1}(m,n) - BIMF_k(m,n) \tag{4}$$

where k is the IMF number.

The sifting process is continued until no more BIMFs are encountered. This happens when $R_k(m,n)$ becomes a constant, monotonic function. The image is reconstructed after summing up all the N decomposed BIMFs and the residue $R_N(m,n)$ which is given by:

$$\tilde{f}(m,n) = \sum_{k=1}^{N} BIMF_k(m,n) + R_N(m,n) \tag{5}$$

2.1.2. Bi-dimensional Ensemble Empirical Mode Decomposition (BEEMD): an overview

Even though BEMD is a useful decomposition tool for texture analysis, it has the following problems: (a) BEMD has the problem of mode mixing. BEMD is a technique to extract modes that can be identified by the sifting process. The BEMD cannot separate the mode in an IMF when a mode does not have even distribution of maxima and minima by the sifting process. (b) Hence a single IMF consists of signals of different scales or the mode will get mixed in another IMF. Thus, BIMFs obtained using BEMD will not be orthogonal to each other due to mode mixing, which is the main drawback in texture analysis.

To overcome the above-mentioned problems of BEMD, a decomposition algorithm called Bi-dimensional Ensemble Empirical Mode Decomposition algorithm was developed which is the 2-D extension of EEMD [23]. The sifting process in BEEMD algorithm is explained as follows:

The I realizations of zero-mean white Gaussian noise is added to the input image $f(m,n)$ which is given by:

$$f^i(m,n) = f(m,n) + \beta w^i(m,n) \tag{6}$$

where $w^i(m,n)$ is the zero-mean white gaussian noise of different realizations from $i = 1, 2, \ldots I$ and β is the standard deviation of the noise. For each i, $f^i(m,n)$ is decomposed into its BIMFs using BEMD to get the modes, $BIMF_k^i(m,n)$ where $k = 1, 2 \ldots K$ are the mode numbers. The k^{th} mode of $f(m,n)$ is obtained by taking the average of $BIMF_k(m,n)$ over I

realizations. It is given by:

$$\overline{BIMF}_k(m,n) = \frac{1}{I}\sum_{i=1}^{I} BIMF_k^i(m,n) \tag{7}$$

The residue is obtained for each of the realizations of the noise as follows:

$$R_k^i(m,n) = R_{k-1}^i(m,n) - BIMF_k^i(m,n) \tag{8}$$

In BEEMD, the decomposition is incomplete because, each $f^i(m,n)$ is decomposed into its BIMFs independent of other realizations of the noise. This leads to reconstruction error since the reconstructed image is obtained by adding all the decomposed BIMFs.

2.1.3. *The proposed modified Bi-dimensional empirical mode decomposition*

Even though the mode mixing problem is overcome in BEEMD, the decomposition in BEEMD is incomplete with high reconstruction error caused by adding different realizations of noise to the signal.

To overcome such incomplete decomposition problem of BEEMD, a decomposition algorithm is proposed in this work called Modified Bi-dimensional Empirical Mode Decomposition (MBEMD). The proposed MBEMD is based on the decomposition algorithm called Complete Ensemble Empirical Mode Decomposition with Adaptive Noise (CEEMDAN) [24]. The proposed MBEMD algorithm is explained as follows:

(i) The first mode, BIMF1 is obtained in the same way as in BEEMD. The first IMF is given by:

$$\overline{BIMF}_1(m,n) = \frac{1}{I}\sum_{i=1}^{I} BIMF_1^i(m,n) \tag{9}$$

where $BIMF_1^i(m,n)$ is the first mode obtained by adding ith realization of white.

Gaussian noise to the input image.

(ii) The first residue is calculated as:

$$R_1(m,n) = f(m,n) - \overline{BIMF}_1(m,n) \tag{10}$$

(iii) Decompose the residue by adding I realizations of white noise w^i and the second mode is obtained as:

$$BIMF_2(m,n) = \frac{1}{I}\sum_{i=1}^{I} BIMF_1[R_1(m,n) + \beta w^i(m,n)] \tag{11}$$

(iv) In equation (11) the noise amplitude β is kept constant irrespective of the realization number. The subsequent residues and BIMFs are obtained as given in equations (12) and (13) respectively.

$$R_k(m,n) = R_{k-1}(m,n) - \overline{BIMF}_k(m,n) \tag{12}$$

$$\overline{BIMF}_k(m,n) = \frac{1}{I}\sum_{i=1}^{I} BIMF_1[R_{k-1}(m,n) + \beta w^i(m,n)] \tag{13}$$

where $k = 1,2\ldots K$ is the number of modes with $i = 1,2\ldots I$, the number of realizations. The step 4 is repeated until the residue is monotonic and constant so that it cannot be decomposed further.

(v) The reconstructed image is obtained by adding all the modes and the residue which is given by:

$$\tilde{f}(m,n) = \sum_{k=1}^{K} \overline{BIMF}_k(m,n) + R(m,n) \tag{14}$$

Equation (14) shows that MBEMD leads to complete decomposition with no or negligible reconstruction error. Also, the mode mixing problem does not occur because of the better separation of the modes. Thus, the number of sifting iterations is reduced, leading to less computational complexity.

2.1.4. *Performance comparison of EMD algorithms*

The decomposition of the mammogram image into its BIMFs using BEMD, BEEMD and the proposed MBEMD is shown in Fig. 2. Four modes are obtained through BEMD and BEEMD: BIMF1, BIMF2, BIMF3 and BIMF4. For MBEMD method of decomposition five modes are obtained.

The last two modes of MBEMD are added (BIMF4, BIMF5) and only four modes are shown in Fig. 2. This is done to have a uniformity in the

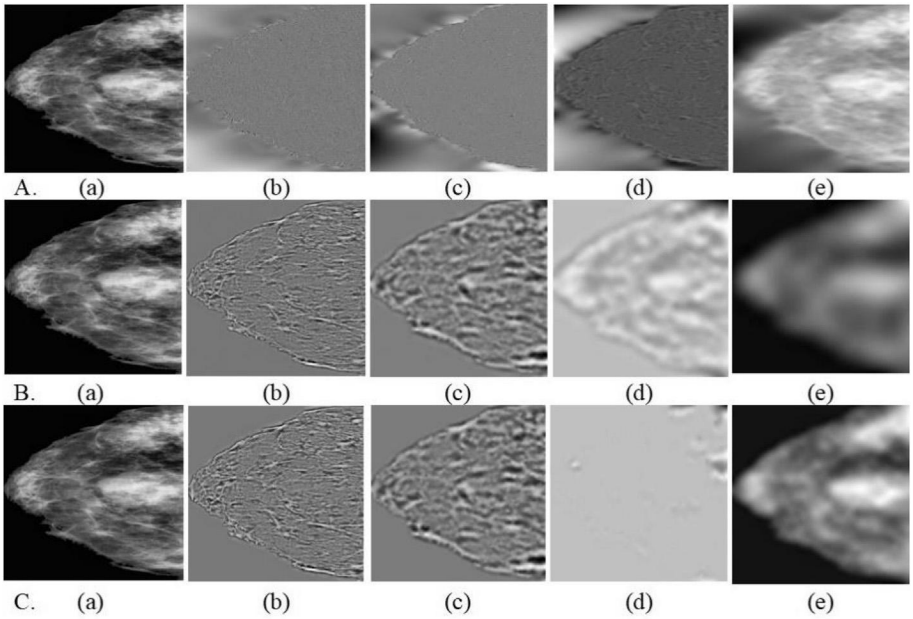

Fig. 2. Decomposition of DDSM image B_3101_1. RIGHT_CC into its BIMFs. A. Decomposition by BEMD B. Decomposition by BEEMD C. Decomposition by the proposed MBEMD. (a) Input image (b) Mode 1: BIMF1 (c) Mode 2: BIMF 2 (d) Mode 3: BIMF3 (e) Mode 4: BIMF4.

displayed images of BEMD, MBEMD modes in the figure. However, for experimental analysis, all the modes are treated individually. Since the sum of the BIMFs and the residue results in the original image, the residue is defined as the last mode. The noise amplitude is selected as $\beta = 0.01$ in our work. The number of realizations is restricted to $I = 50$ reduce the computational cost.

The performance of the decomposition algorithm is evaluated by the parameters: (i) Orthogonality Index (ii) Peak Signal to Noise Ratio (PSNR) (iii) Mean Square Error.

(i) Orthogonality Index (OI): The efficiency of the decomposed algorithm is evaluated by the orthogonality of the decomposed IMFs. The IMFs should be orthogonal to each other which shows the completeness of the decomposition algorithm. The lower the orthogonality, the lesser the amount of leakage between the IMFs. The Orthogonality Index (OI) [22] is given for the image $f(m,n)$ as:

$$OI = \sum_{m=1}^{M}\sum_{n=1}^{N}\left(\sum_{i=1}^{K+1}\sum_{j=1}^{K+1}\frac{BIMF_i(m,n)BIMF_j(m,n)}{f^2(m,n)}\right) \tag{15}$$

where MxN is the size of the image with M rows and N columns. $BIMF_i(m,n), BIMF_j(m,n)$ with $i,j = 1,2\ldots K$ are BIMFs and $BIMF_{K+1}(m,n)$ is the residue. Hence residue can be considered as last mode.

(ii) Mean Square Error (MSE)**:** It is defined as the average of the square of the error between original image $f(m,n)$ and the reconstructed image $\tilde{f}(m,n)$ with M rows and N Columns. The reconstructed image is obtained by adding all BIMFs. MSE is given by the following equation:

$$MSE = \frac{1}{MN}\sum_{m=1}^{M}\sum_{n=1}^{N}[f(m,n) - \tilde{f}(m,n)]^2 \tag{16}$$

(iii) Peak Signal to Noise Ratio (PSNR): PSNR of the image $f(m,n)$ refers to the ratio of maxthe imum value of intensity f_{max} in an image to its mean square error (MSE) value that is defined by:

$$PSNR = 10log_{10}\left[\frac{f_{max}}{MSE}\right] \tag{17}$$

To evaluate the proposed MBEMD method, mammogram images from MIAS, DDSM and MGM hospital are decomposed into BIMFs using BEMD and the proposed MBEMD. For every image from each of these databases, OI between IMFs, MSE and PSNR values of the reconstructed image are computed for both BEMD and proposed MBEMD technique and the average of OI, MSE and PSNR are given in Table 1. The efficiency of the decomposition depends on OI which should be low. From Table 1, it is seen that OI is high in BEMD and hence mode mixing problem is predominant. Also, MSE is less to show the completeness of BEMD algorithm. In BEEMD method, the average OI is lesser than BEMD and hence the mode mixing problem is overcome. But, however, the average MSE is high, which shows that the decomposition is incomplete resulting in low PSNR. The singular disadvantages of mode mixing in BEMD and incomplete decomposition in BEEMD are overcome in the proposed decomposition algorithm MBEMD.

The quality of BIMFs is also affected by noise amplitude which is added during the decomposition stage in BEEMD and MBEMD. When noise amplitude is increased for a specific ensemble size, the reconstruction error which is the difference between the input image and sum of the BIMFs also increases. A complete empirical mode decomposition is said to be attained, only if the reconstruction error is very less. If complete decomposition is not achieved then the extracted features from the incompletely decomposed BIMFs would fail to yield perfect texture features. Hence an experiment is conducted by varying noise amplitude with standard deviation σ between 0.001 and 0.1. We found that for the noise amplitude with $\sigma = 0.01$, good quality BIMFs with acceptable MSE is obtained. The effect of noise amplitude on MSE along with other performance metrics is shown in Table 1. The results prove that the proposed MBEMD algorithm is suitable for texture analysis. It is to be recalled that in the BEMD algorithm no random noise is added.

2.1.5. *Illustration of mode mixing problem*

The main drawback of BEMD is mode mixing problem, a single BIMF consists of signals of other modes or a single-mode present in more than one BIMF. This results in overlapping of modes in distinct spatial frequencies. Whereas, in the proposed MBEMD method, the mode mixing problem is reduced and better spectral separation of modes is achieved. This is because, at each of stage of MBEMD, a specific noise is added leading to unique mode. The problem of mode mixing is well understood by finding radially averaged power spectral density for every BIMF obtained through BEMD/MBEMD which is illustrated in Fig. 3. From Fig. 3, it reveals that in BEMD, the modes are overlapped in spatial frequencies, leading to the mode mixing problem. The spectral mode separation in MBEMD is better than in BEMD. Also, better mode alignment is achieved at higher spatial frequencies for MBEMD modes. Hence, more distinct features can be extracted from each of these modes, leading to better mammogram mass classification.

2.2. *Pre-processing*

Pre-processing of mammogram images is the first step and must be done to enhance the quality of the image to improve the classification accuracy in the diagnosis of breast masses. In the pre-processing step, image enhancement is performed based on Contrast Limited Adaptive Histogram Equalization (CLAHE) followed by Gaussian smoothing.

2.2.1. *CLAHE based enhancement*

In CLAHE algorithm, the image is divided into non-overlapping regions of equal sizes. These non-overlapping regions are called contextual region. For each of these contextual regions, the histogram is calculated. A predetermined threshold is set and the histogram of each of these regions is modified so that its height does not exceed the threshold. The

Table 1
Performance comparison of Decomposition algorithms for mammogram images.

Decomposition Method	Mammogram database	OI	MSE			PSNR
			σ = 0.005	σ = 0.01	σ = 0.1	
BEMD	MIAS	0.1568	–	–	–	374.45
	DDSM	0.0989	–	–	–	373.82
	MGM Hospital	0.1326	–	–	–	374.23
BEEMD	MIAS	0.0411	3.34E-08	4.99E-06	3.09	101.14
	DDSM	0.0417	2.58E-07	4.98E-06	2.17	101.17
	MGM Hospital	0.0658	3.01E-08	5.01E-06	2.65	101.13
Proposed MBEMD	MIAS	0.019	2.12E-35	2.15E-34	3.47E-8	384.83
	DDSM	0.02	2.17E-35	2.07E-34	2.16E-7	385.15
	MGM Hospital	0.0387	1.92E-36	2.95E-34	2.56E-7	383.43

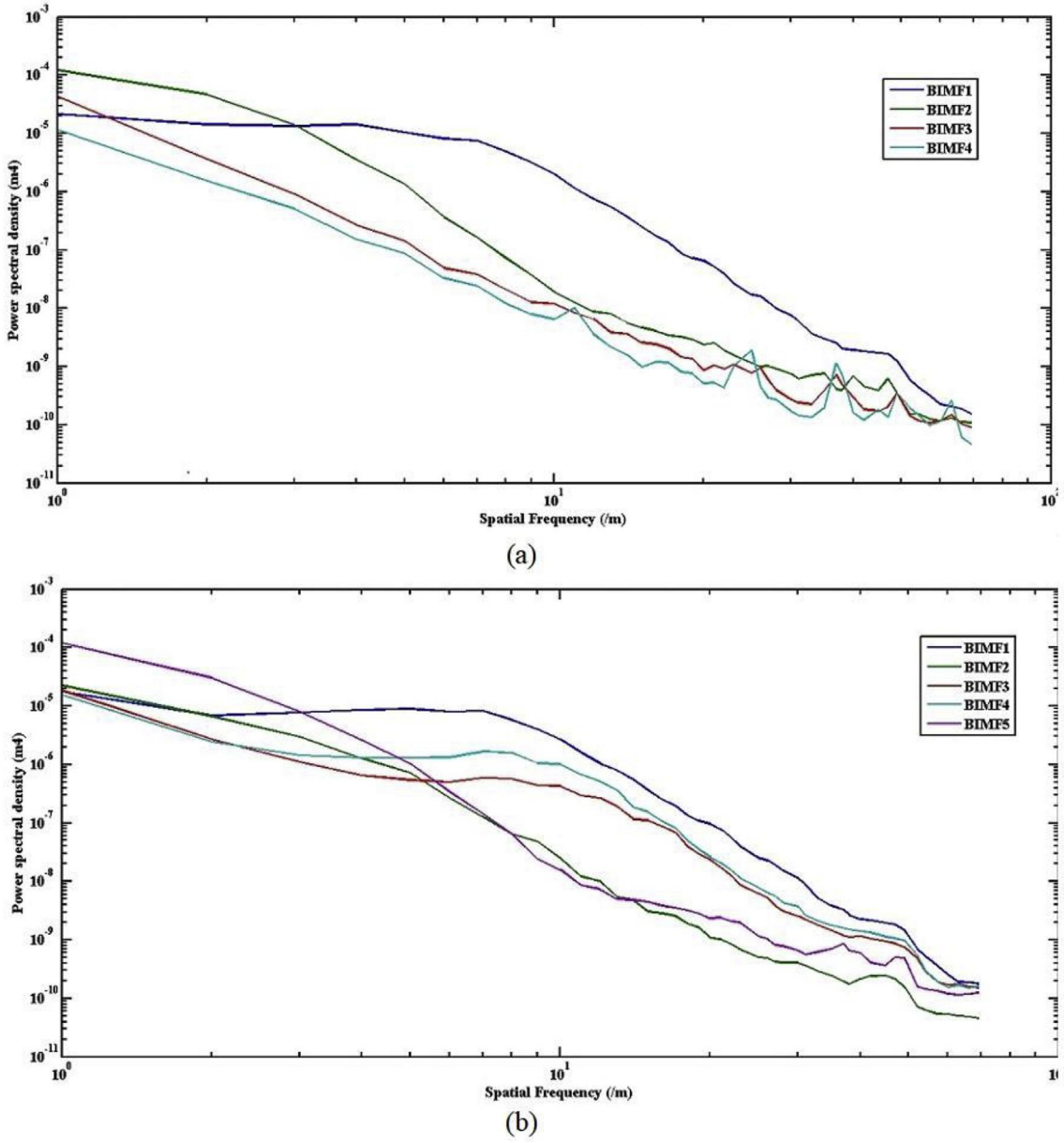

Fig. 3. Illustration of mode mixing: (a) BEMD (b) MBEMD.

gray scale values are changed according to the modified histogram [25].

2.2.2. *Gaussian smoothing*

Low pass Gaussian filter is used to smoothen the image. The image smoothing is performed in the frequency domain. The Fourier transform of the image and that of the Gaussian filter is multiplied pixel by pixel. By taking inverse Fourier transform of the resultant image, smoothing is achieved [26]. Image enhancement based on CLAHE and Gaussian smoothing are shown in Fig. 4.

2.3. *ROI extraction*

To implement the proposed feature extraction technique in mammogram images, the ROI must be extracted from the entire image, otherwise leads to undesirable results. There are two types of lesions in mammograms: masses and microcalcifications. Detection and diagnosis of masses is a challenging task because the shape and size of the masses are instable. Also, some masses have poor contrast and are overlapped with normal breast tissues. A low density, round or oval shape, well-defined margin masses are generally categorized as benign, whereas masses with high density, spiculated margin and ill-defined shape are categorized as malignant [11]. In this work, ROI is the suspicious mass in mammogram image that is extracted from the pre-processed image by manual cropping.

2.4. *The proposed method of feature extraction*

In the proposed method, texture features are extracted using two EMD techniques: (i) BEMD based feature extraction (ii) MBEMD based feature extraction. BIMFs that are obtained after decomposing the ROI of mammogram using BEMD and the proposed MBEMD method strongly characterize the texture features of the mammogram image. For each of these BIMFs, five GLCM features and seven GLRM features are extracted, which are given as input to the classification stage to classify the ROI into benign or malignant. The classifiers employed in this work are SVM and LDA classifiers. In our work, we have not implemented BEEMD for

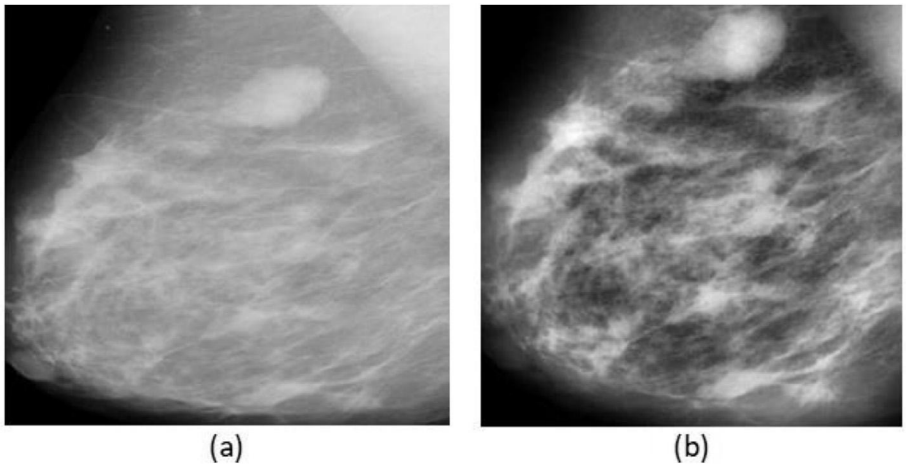

Fig. 4. Image Enhancement (a) Input MIAS image mdb015 (b) Enhanced image after CLAHE and Gaussian smoothing.

feature extraction because the decomposition in BEEMD is not complete.

2.4.1. BEMD based feature extraction

The ROI of the mammogram image is decomposed into its BIMFs using BEMD method of decomposition. These BIMFs are called modes. Four modes are obtained by applying BEMD on ROI of mammogram image. Fig. 5 shows the BIMFs extracted from ROIs of mammogram images using BEMD technique. After the decomposition of mass ROI into its BIMFs or modes, texture features are to be extracted from each of these BIMFs. Texture features have the information about a region's structural arrangement in an image and the relationship between the adjacent or sounding regions. The extracted features can be used for the classification of suspicious ROI into benign or malignant.

In this work, combined GLCM and GLRLM based features [15] are extracted from BIMFs of mammogram ROI. The texture analysis of images was based on first order or second-order statistics of textures. Even though many techniques like Gabor filter, Fractals, Wavelet transform have been used for texture analysis, the most efficient technique is Gray Level Co-Occurrence Matrix (GLCM) based features. GLCM is a 2-D matrix which identifies specific texture in an image by modeling texture as gray level variation. GLCM was based on second-order statistics of textures of the image. The elements in the GLCM array correspond to the frequencies of variation of pixel intensity in an image. Haralick RM et al. [27] extracted 14 features from GLCM. Out of these, five common features Energy, Contrast, Entropy, Maximum Probability (Max. Prob) and Inverse Difference moment (Inv. Diff) have been used in this work.

Gray Level Run Length Matrix (GLRLM) is a 2-D array whose elements corresponds to the number of adjacent pixels with the same intensity in a particular direction. GLRLM is given by $f(i,j|\theta)$, where each element j in the matrix is the number of times, intensity i occurs in the image in a particular direction θ. Seven texture features are extracted from this matrix. The seven texture features are Short Run Emphasis (SRE), Long Run Emphasis (LRE), Gray Level Non-uniformity (GLN), Run Percent (RP), Run Length Non-uniformity (RLN), Low Gray level Run Emphasis (LGRE) and High Gray level Run Emphasis (HGRE) [15]. The combined 12 features of GLCM and GLRLM are obtained from the extracted BIMFs of the ROI of mammogram image.

2.4.2. MBEMD based feature extraction

By investigating Fig. 5, it is clear that every mode of each of the ROI shows different texture. However, in BEMD some frequency components of a particular scale are available at other scales which is called mode mixing. Hence texture information of a particular mode is available in other modes, leading to high OI between the modes. The GLCM, GLRLM features extracted from the mode mixed BIMFs of the ROI, has a great impact on the diagnostic accuracy in the classification of masses and it is shown in experimental results. To overcome this problem, the features are extracted from the BIMFs obtained by applying the proposed MBEMD technique on mammogram ROI. The BIMFs extracted from ROIs of mammogram images using MBEMD technique is shown in Fig. 6. Similar to BEMD based feature extraction, 12 combined features from GLCM and GLRLM are obtained and these features are given as input to the classifier for the classification into benign or malignant.

2.4.3. Performance evaluation of BEMD and the proposed MBEMD based feature extraction

In the proposed method of feature extraction, the ROI is decomposed into its BIMFs using BEMD and the proposed MBEMD techniques. The GLCM-GLRLM feature values from each of these BIMFs are obtained. From the MIAS database, 92 ROIs consisting of both benign and malignant masses are decomposed using BEMD and the proposed MBEMD. The combined twelve features from GLCM-GLRLM are extracted from each of the modes (BIMFs) obtained by decomposing the mammogram ROIs. Similarly, GLCM-GLRLM features are extracted from 120 ROIs of the DDSM database and 88 ROIs of MGM hospital database.

In order to verify the class discrimination of the extracted features, Kruskal-Wallis statistical test has been implemented on BEMD/MBEMD features of randomly selected mammogram ROIs. These ROIs consist of both benign and malignant masses. Fig. 7–10 shows the results of a statistical test applied for BIMF1 (mode 1) of BEMD and the proposed MBEMD based feature extraction for the MIAS database. Out of twelve features extracted from BIMFs, the most significant features are shown in these figures. The GLCM-contrast feature distribution for BEMD and MBEMD are (benign: 0.5–1.5, malignant:1.5–2.9), (benign:0.7–2.2, malignant:0.1–0.2) respectively. Similarly, the feature distribution for GLCM-Energy, GLRLM-GLN, GLRLM-HGRE are shown in Figs. 7–10. It is seen from the figures that MBEMD based features have distinct feature measures of Energy, Contrast, GLN and HGRE for benign and malignant ROIs, whereas BEMD based features are overlapped for benign and malignant ROIs. In specific, GLRLM-GLN feature distribution of BEMD for benign is 2.5–3 and for malignant is 0.05–4.5, which are completely overlapped resulting in poor class discrimination. This shows that MBEMD based feature extraction has distinguished significance of discrimination between benign and malignant classes.

2.5. Mass classification

The extracted features from the decomposed ROIs of mammogram images are given as input to the classifier to classify the suspicious ROIs into benign or malignant. SVM and LDA classifiers are used for mass classification in this work.

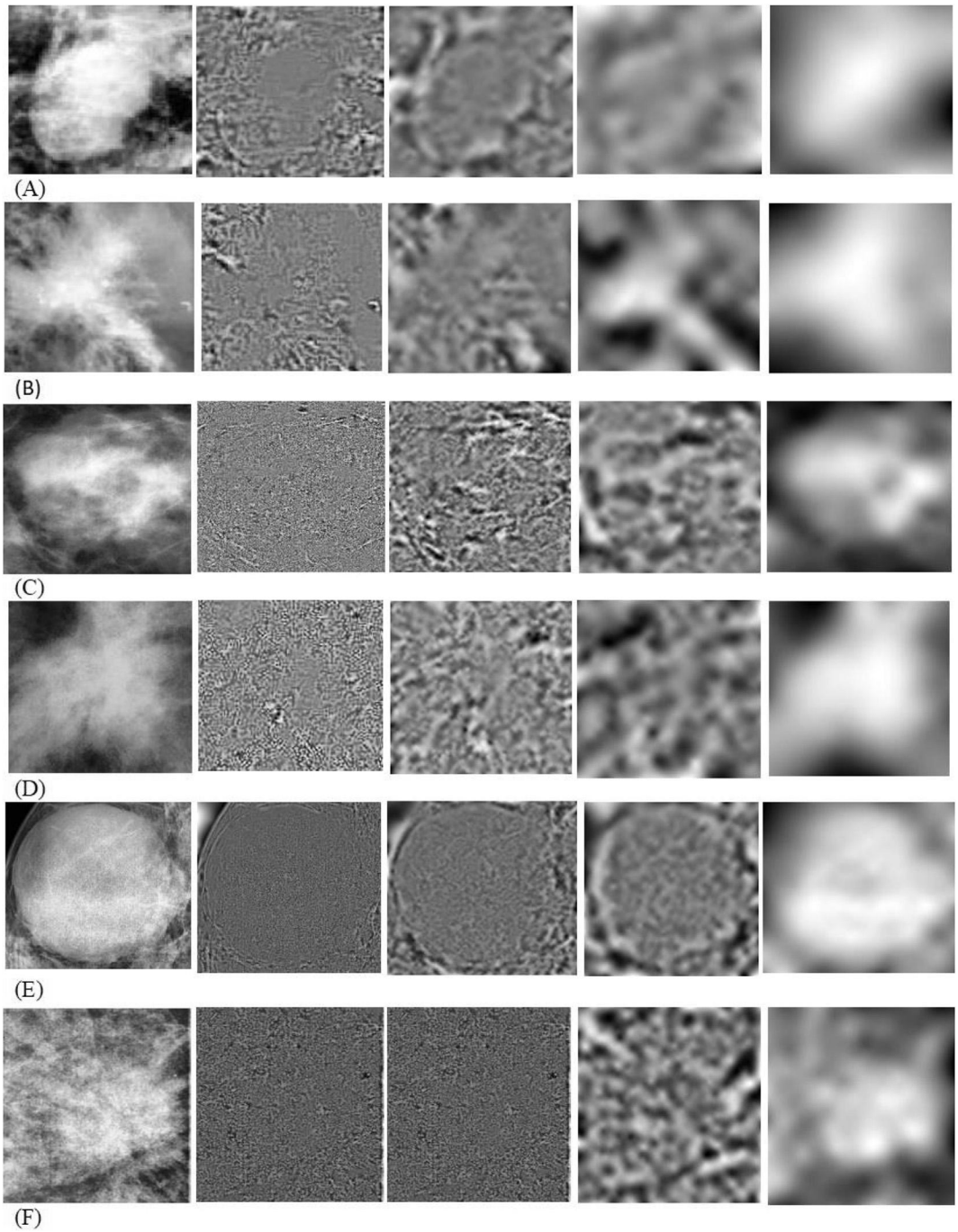

Fig. 5. BIMFs extracted from ROIs of mammogram images using BEMD method. The first column shows input ROIs. The next successive columns show BIMFs extracted from the corresponding ROIs. A. MIAS image mdb170. B. MIAS image mdb032. C. DDSM image B_3101_1. RIGHT_CC D. DDSM image C_0001_1.RIGHT_CC. E, MGM hospital images. A, C, E are benign masses and B, D, F are malignant masses.

2.5.1. SVM classifier

The Support Vector Machine (SVM) Classifier is based on statistical learning theory. SVM is used for classification in applications that do not need a large training data set. Linear discrimination is achieved in SVM, in which a hyperplane is calculated to separate the feature samples into different classes. The hyperplane is calculated in such a way that the distance between the marginal feature samples of data of each class is maximized. Thus, the optimization problem consists of (i) finding hyperplane for separation of samples into classes. (ii) Maximizing the distance between the marginal feature samples of each class. The solution to this optimization problem is provided by the small percentage of marginal samples called Support Vectors. The distance of a feature sample from the hyperplane is given by the decision function:

$$\widehat{f}(x) = b + \sum_{i=1}^{n} \propto_i y_i K(x_i, x) \; ; \; y_i \in [0, 1] \tag{29}$$

where $i = 1, 2, \ldots n$ are the multipliers which are non-zero for the support vectors, b is a bias value, $\propto$ is a weight vector, $K(x_i, x)$ is a kernel function [28] and x_i is the input feature vector. In this work.

2.5.2. LDA classifier

In LDA, optimal transform is found by minimizing the distance of within-class sample features and maximizing the distance of between-

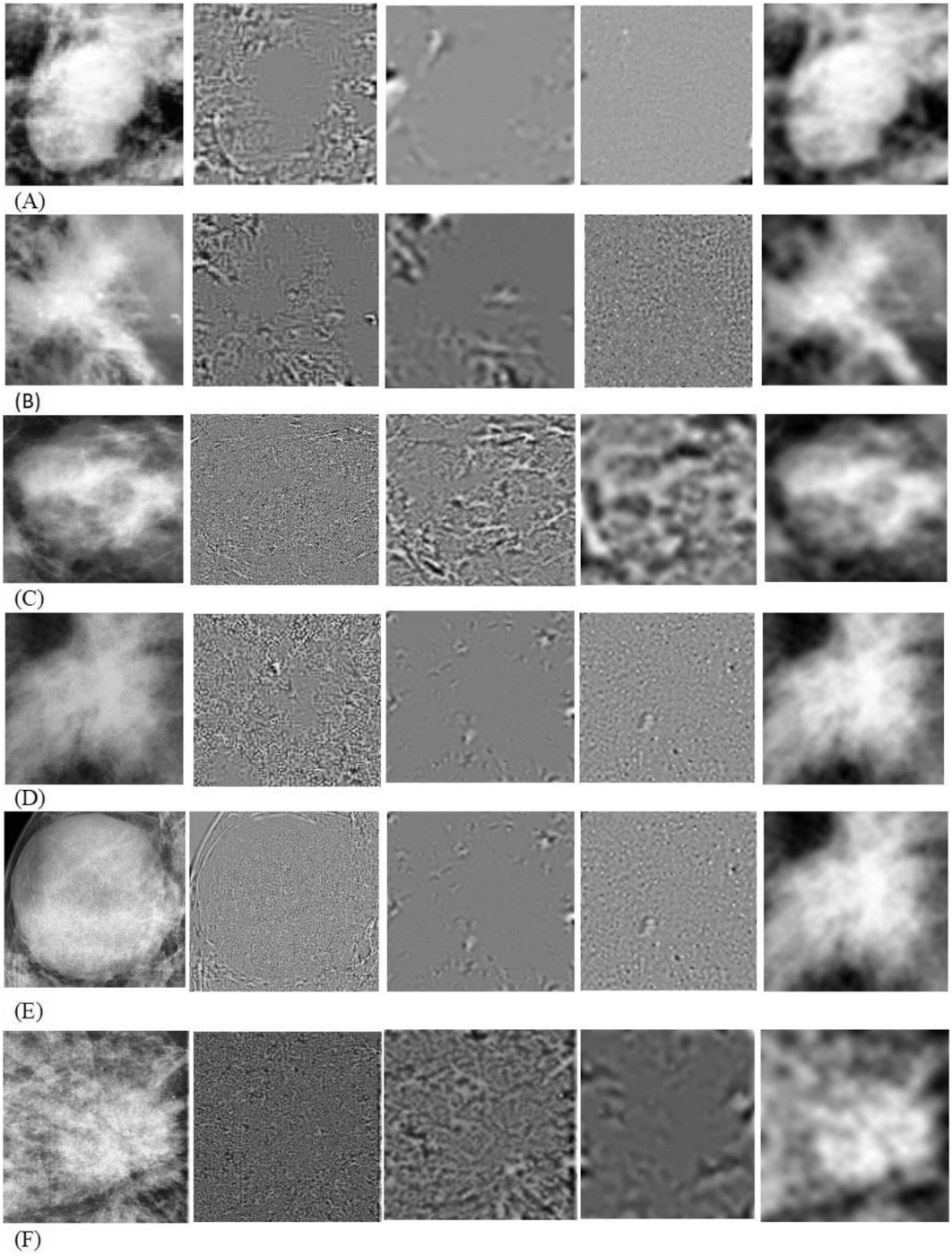

Fig. 6. BIMFs extracted from ROIs of mammogram images using the Proposed MBEMD method. The first column shows input ROIs. The next successive columns show BIMFs extracted from the corresponding ROIs. A. MIAS image mdb170. B. MIAS image mdb032. C. DDSM image B_3101_1. RIGHT_CC D. DDSM image C_0001_1.RIGHT_CC. E, MGM hospital images. A, C, E are benign masses and B, D, F are malignant masses.

class sample features simultaneously. LDA is based on the concept of looking for a linear combination of input variables or predictors that can provide the best separation between the classes (targets) [29].

3. Experimental results

The proposed feature extraction method is evaluated on the mammogram images collected from MIAS database, DDSM database and local database (MGM hospital images). The entire mammogram ROIs are divided into two non-overlapping data set for training and testing. Table 2 gives the details of the ROIs used for training and testing. The classification results of MGM hospital images were verified by the radiologist.

3.1. Parameterization of classifier

In SVM, determination of hyperplane and maximization of the distance between each class marginal features are given by:

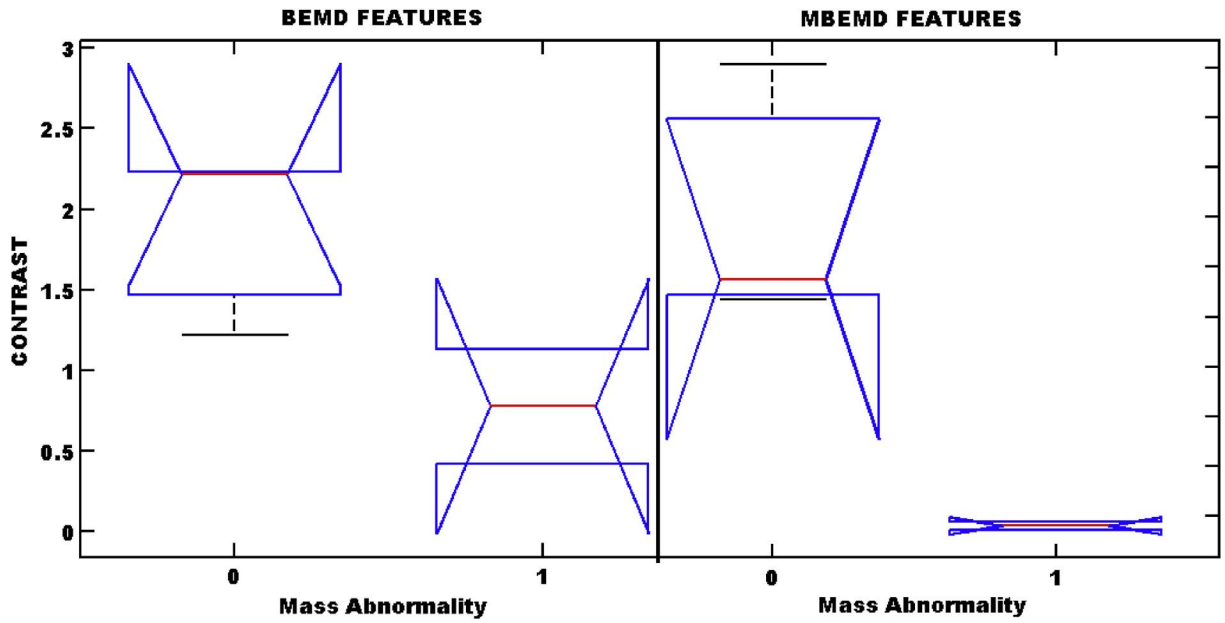

Fig. 7. GLCM - Contrast feature value distribution for Benign (0) and Malignant (1) masses obtained by BEMD and MBEMD based Feature extraction method.

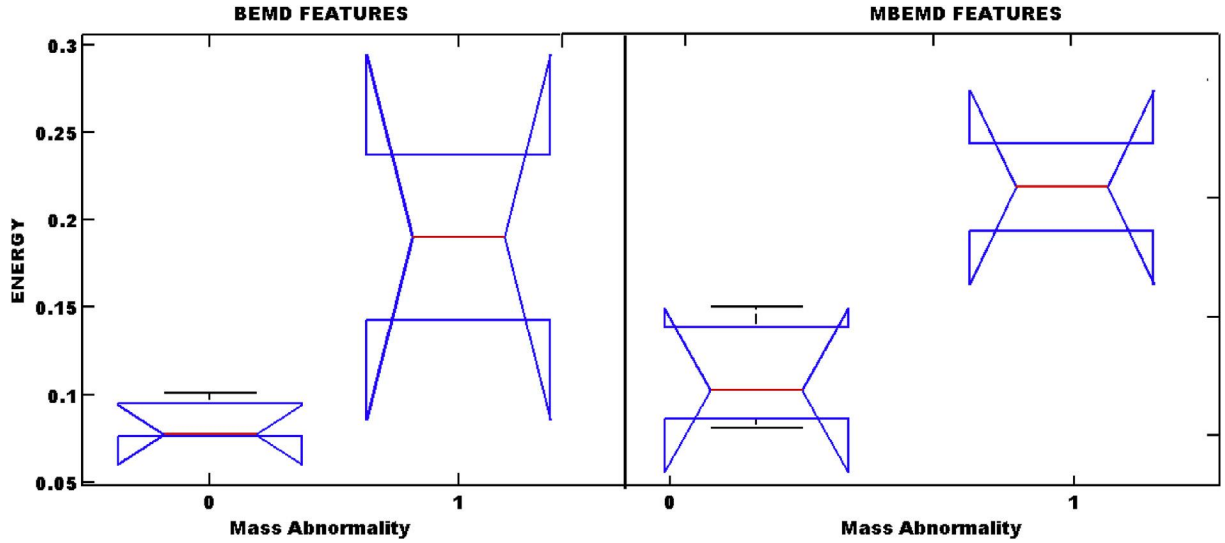

Fig. 8. GLCM - Energy feature value distribution for Benign (0) and Malignant (1) masses obtained by BEMD and MBEMD based Feature extraction method.

$$\min_{w,b,\tau} \frac{1}{2}\alpha, \alpha + C^{+}\sum_{i\in+}\tau_i + C^{-}\sum_{i\in-}\tau_i \tag{30}$$

subject to $y_i(\alpha, \varnothing(x)_i + b) \geq 1 - \tau_i; \tau_i \geq 0$; where. $K(x, x^{'}) = \varnothing(x)^T \varnothing(x)^{'}$

The mapping function $\varnothing(x)$ is used to project the data in order to obtain the non-linear decision boundaries. In order to perform classification for the given test sets, parameters of the classifier have to be determined. In LDA, all required parameters were estimated from the training set and hence LDA is applied directly for the test sets. In SVM, if the feature vectors are inseparable, then the penalty term C, with C^{+} for the negative class and C^{-} for the positive class is used to control the misclassification errors during training and the kernel 'σ', controls the effect of support vectors on decision boundary. In our work, we have taken $C^{+} \in \{1, 10, 25, 75, 100\}$ and $C^{-} := 1$. The Gaussian kernel width is chosen as $\sigma \in \{0, 0.25, 0.5, 0.75\}$. During cross-validation, optimum results are obtained for parameters $C^{+} = 10$ and $\sigma = 0.5$.

A feature vector is constructed by computing twelve GLCM-GLRLM features from each of the BIMFs obtained by decomposing ROIs using BEMD and the proposed MBEMD methods. This feature vector is given as input to SVM and LDA classifiers for classification. The metrics used for evaluating the classification performance are (i) Accuracy (ii) AUC of ROC. Accuracy is defined as the ratio of the number of ROIs classified correctly to the total number of ROIs available in mammogram ROIs. ROC is the plot of True Positive Rate (TPR) drawn as the function of False Positive Rate (FPR).

After performing ten folds of cross validation, the average accuracy and AUC of SVM classifier to classify the ROIs into benign and malignant is given in Table 3 and that of LDA classifier is shown in Table 4. From Tables 3 and 4 it is seen that classification accuracy of BIMF1 features is high compared to other BIMFs. This is because the edge information is present in lower modes which correspond to higher spatial frequencies. Also, the highest classification accuracy of MBEMD based features have been achieved with AUC closer to 1.

From Table 3 and 4 it is seen that the performance of SVM is better than LDA due to the choice of penalty parameters that can be changed

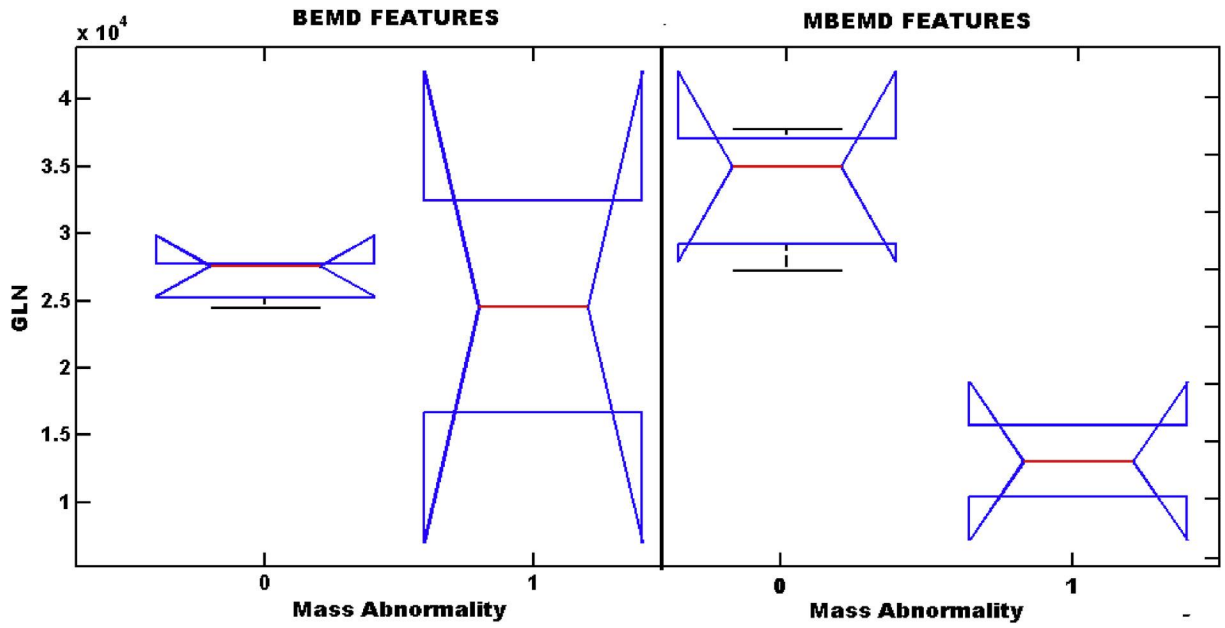

Fig. 9. GLRLM-GLN feature value distribution for Benign (0) and Malignant (1) masses obtained by BEMD and MBEMD based Feature extraction method.

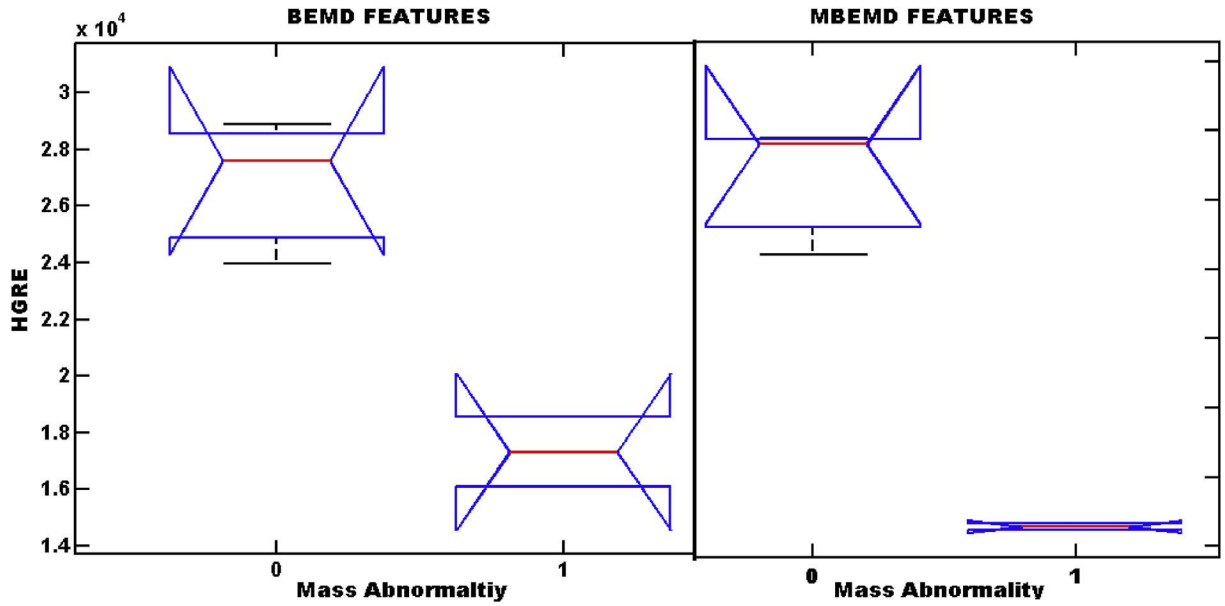

Fig. 10. GLRLM-HGRE feature value distribution for Benign (0) and Malignant (1) masses obtained by BEMD and MBEMD based Feature extraction method.

Table 2
ROIs with masses used for the evaluation of proposed feature extraction.

Database	Abnormality Type	Total No. of ROIs	No. of Training Sets	No. of Testing Sets
MIAS	Benign	53	38	15
	Malignant	39	27	12
DDSM	Benign	60	45	15
	Malignant	60	45	15
MGM	Benign	59	40	19
Hospital	Malignant	29	18	11

when misclassification error occurs. SVM classifier shows superior performance for both BEMD and MBEMD features, than LDA classifier.

The ROC curves obtained with SVM and LDA classifiers for BIMF1 features of MIAS database is shown in Fig. 11. The more the ROC curve touches the upper right panel, the better the classification accuracy. Hence, it is clear that the proposed MBEMD based feature extraction method with SVM classifier achieves highest accuracy. Similarly, the ROC curves for the DDSM database and MGM hospital database are obtained and are shown in Figs. 12 and 13 respectively. It is seen that irrespective of mammogram database, the proposed MBEMD based feature extraction method performs better than the BEMD based feature extraction technique. Also, the mass classification results show that the performance of SVM classifier is better than LDA classifier.

The performance comparison between SVM and LDA classifiers with BEMD and proposed MBEMD features for MIAS, DDSM and MGM hospital database in terms of accuracy is shown in Fig. 14. It is seen that the classification accuracy is achieved higher with SVM classifier than with LDA classifier.

Table 3
Performance Evaluation of Proposed Feature Extraction method with SVM classifier.

Feature Extraction Method	BIMFs	Performance Metrics	MIAS	DDSM	MGM Hospital
BEMD based Features	BIMF1	Accuracy	88.88%	90%	86.66%
		AUC	0.9	0.90	0.856
	BIMF2	Accuracy	81.48%	83.33%	83.3%
		AUC	0.816	0.83	0.83
	BIMF3	Accuracy	81.48%	83.33	80%
		AUC	0.825	0.83	0.842
	BIMF4	Accuracy	74.07%	76%	73.3%
		AUC	0.741	0.76	0.77
Proposed MBEMD based Features	BIMF1	Accuracy	**96.2%**	**93.33%**	**90%**
		AUC	**0.966**	**0.933**	**0.92**
	BIMF2	Accuracy	85%	86.6%	83.3%
		AUC	0.858	0.866	0.83
	BIMF3	Accuracy	81.48%	83.33%	76%
		AUC	0.825	0.833	0.758
	BIMF4	Accuracy	81.48%	80%	73.3%
		AUC	0.816	0.8	0.712

Table 4
Performance Evaluation of Proposed Feature Extraction method with LDA classifier.

Feature Extraction Method	BIMFs	Performance Metrics	MIAS	DDSM	MGM Hospital
BEMD based Features	BIMF1	Accuracy	88.8%	86.6%	83.3%
		AUC	0.89	0.866	0.83
	BIMF2	Accuracy	88.8%	86.6%	83.33%
		AUC	0.89	0.86	0.81
	BIMF3	Accuracy	77.7%	76.6%	73.33%
		AUC	0.775	0.76	0.732
	BIMF4	Accuracy	70.37%	66.6%	70%
		AUC	0.7	0.66	0.75
Proposed MBEMD based Features	BIMF1	Accuracy	**92.59%**	**90%**	**90%**
		AUC	**0.933**	**0.9**	**0.9**
	BIMF2	Accuracy	85.18%	86.6%	86.6%
		AUC	0.85	0.866	0.875
	BIMF3	Accuracy	81.48%	76.6%	73.3%
		AUC	0.825	0.766	0.693
	BIMF4	Accuracy	74.07%	70%	70%
		AUC	0.741	0.7	0.667

3.2. Comparison with other methods

The performance of the proposed method is compared with other state-of-the-art methods in the literature in terms of average accuracy and AUC of ROC. The dataset and the number of ROIs used for the proposed method is different from those used by the other methods. Hence a fair comparison is made by compiling information from other methods in the literature and is given in Table 5. The comparison results in this table convey that the proposed feature extraction method is robust. This means that the overall performance of the system is relatively consistent when applied across different databases. Even though some other existing feature extraction methods given in Table 5 yield superior results, the consistency in the performance by testing with different databases is not shown which is essential for any CAD system.

Even though there are many modern methods such as deep learning networks are available for mammogram mass classification, these base line methods are not used in this work for the following reasons:

(i) A massive amount of data is required to train a deep learning network. In this work, we have shown that the proposed method is efficient when applied across different databases with less volume of data set [30–32].
(ii) Training a deep learning network is time consuming which takes days or weeks even if modern Graphics Processing Units are used for this. Whereas, our work is less time consuming and can be been implemented in any available Central Processing Units [33–36].
(iii) The deep learning network such as convolutional neural network could not provide better classification if the training data size is small [30–32,37,38].

In our work, we have implemented hand-crafted features based on BEMD and MBEMD and achieved with optimum results.

4. Conclusion

In this paper, two feature extraction methods based on BEMD and the proposed decomposition method called MBEMD for the classification of masses in mammogram images are presented. The results show that the proposed method has several advantages over other state-of-the-art-methods: first, BEMD or MBEMD does not require any basis function and it is completely data-driven. which differs from transform based feature extraction methods. The results show that decomposition in the proposed MBEMD method is complete and the extracted modes are orthogonal to each other. Hence different texture features are extracted

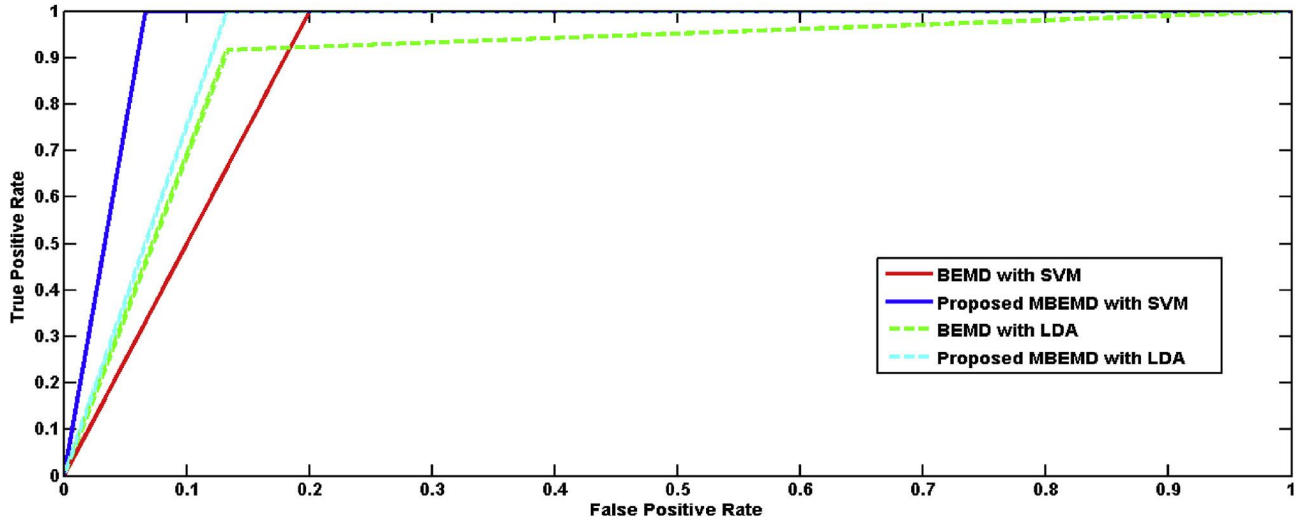

Fig. 11. Comparison of the ROC curves between BEMD and the proposed MBEMD features with SVM and LDA classifiers for MIAS database.

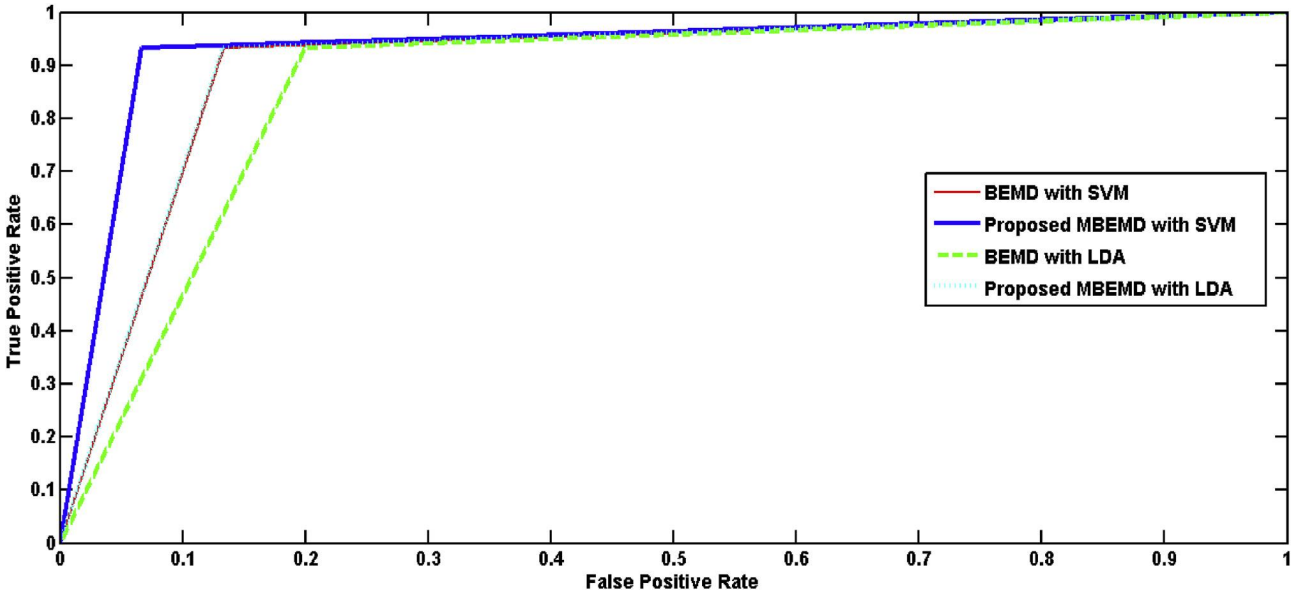

Fig. 12. Comparison of the ROC curves between BEMD and the proposed MBEMD features with SVM and LDA classifiers for the DDSM database.

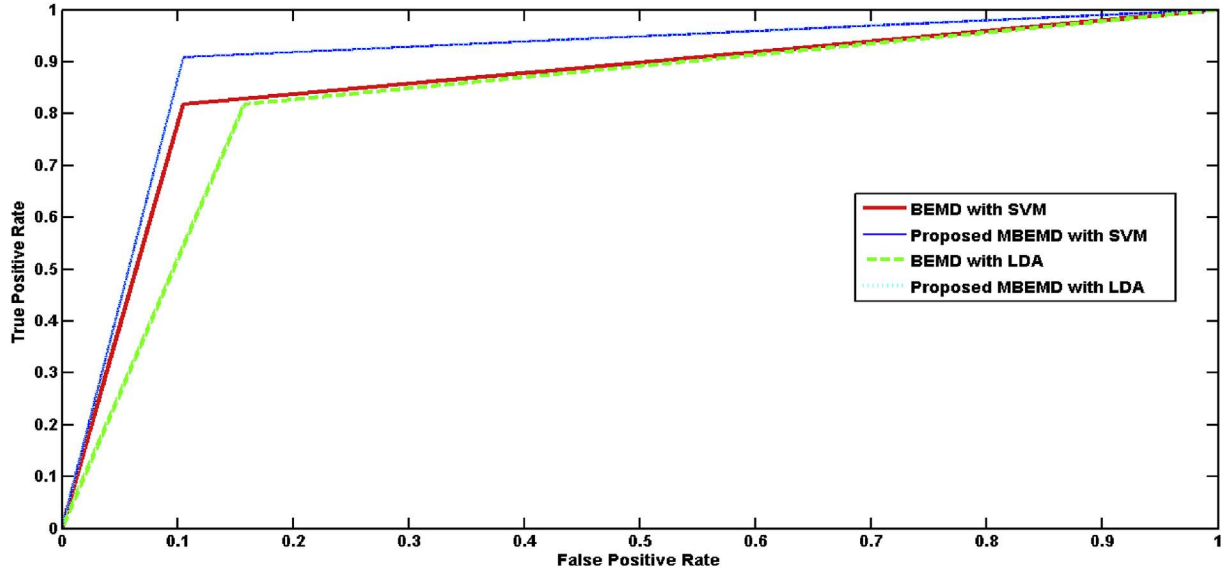

Fig. 13. Comparison of the ROC curves between BEMD and the proposed MBEMD features with SVM and LDA classifiers for MGM Hospital database.

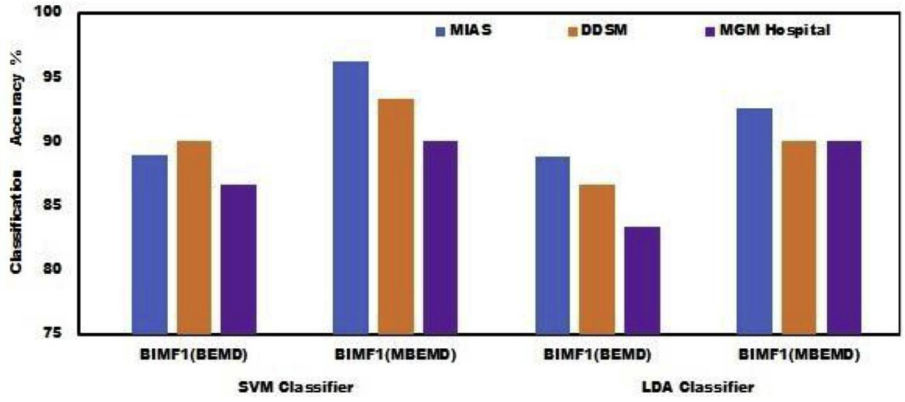

Fig. 14. Comparison between SVM and LDA classifiers in terms of accuracy for MIAS, DDSM, MGM hospital database.

Table 5
Comparison of the proposed feature extraction with other existing methods.

Feature Extraction Methods	Database	No. of ROIs	Average Accuracy in %	AUC
Contourlet transform [17]	MIAS	90	87.00 ± 0.008	–
Gabor wavelets [16]	MIAS	114	78.26	0.78
Geometry and texture features [13]	DDSM	826	94	0.9615
Gabor filters [12]	DDSM	512	93.95 ± 3.85	0.948 ± 0.043
Structural similarity mapping [11]	MIAS	58	94.57	0.98
	DDSM	500	85.42	0.93
Proposed MBEMD method	MIAS	92	96.2	0.966
	DDSM	120	93.33	0.93
	MGM (Local Hospital)	88	90	0.92

in each mode and hidden textures are identified better than in BEMD method which makes it suitable for texture analysis. Second, the accuracy in classifying between benign and malignant masses is higher in the proposed method than other existing methods. Third, class discrimination is achieved with a minimum feature set, thus feature selection is not necessary for this method. The main significance of the proposed system is that the performance of the proposed feature extraction method is consistent when applied for different databases. In this paper, masses in mammograms are classified into benign or malignant. The other type of lesion, microcalcification is not considered in this work. Classification of both masses and microcalcification in mammograms is the next objective of our future research work.

Author's contributions

Vaijayanthi Nagarajan: Conceptualization, Methodology, Software, Data curation, Writing-Original draft preparation. Elizabeth Caroline: Investigation, Visualization, Supervision, Writing-reviewing and editing. Senthilvel Murugan Veeraputhiran: Resources, Supervision and Validation.

Conflict of interest

The authors declare that there are no conflicts of interest.

References

[1] Website National Institute of cancer Prevention and research, "statistics". NICPR; 2019 [Online]. Available: http://cancerindia.org.in/statistics/.
[2] New Global Cancer Data. GLOBOCAN 2018,"Percentage of new cancer cases and cancer deaths world wide in 2018. 12 Septemer. 2018 [Online]. Available: https://www.uicc.org/news/new-global-cancer-data-globocan-2018.
[3] Hu K, Gao X, Li F. Detection of suspicious lesions by adaptive thresholding based on multiresolution analysis in mammograms. IEEE Trans. Instrum. Meas. 2011;60(2):462–72.
[4] Nithya R, Shanthi B. Comparative study on feature extraction method for breast cancer classification. J Theor Appl Inf Technol 2011;12:220–6.
[5] Eltonsy N, Tourassi G, Elmaghraby A. A concentric morphology model for the detection of masses in mammography. IEEE Trans Med Imaging 2007;26:880–9.
[6] Delogu P, et al. Characterization of mammographic masses using a gradient-based segmentation algorithm and a neural classifier. Comput Biol Med 2007;37:1479–91.
[7] Kim D, Lee S, Ro Y. Mass type specific sparse representation for mass classification in computer-aided detection on mammograms. Biomed Eng Online 2012;12:1–13.
[8] Tralic D, Bozek J, Grgic S. Shape analysis and classification of masses in mammographic images using neural networks. In: 18th International Conference on Systems, Signals and Image Processing. Bosnia-Herzegovina; 2011.
[9] Bouguila T, Elguebaly N. "Bayesian approach for the classification of mammographic masses," in Developments in eSystems Engineering. Abu Dhabi: DeSE); 2013.
[10] Cascio D, et al. Mammogram segmentation by contour searching and mass lesions classification with neural network. IEEE Trans Nucl Sci 2006;53:2827–33.
[11] Rabidas R, Midya A, Chakraborty J. Neighborhood structural Similarity mapping for the classification of masses in mammograms. IEEE J. Biomed. Health Inf. 2018;22(3):826–34.
[12] Khan S, et al. Optimized Gabor features for mass classification in mammography. Appl Soft Comput 2016;44:267–80.
[13] Liu X, Tang J. Mass classification in mammograms using selected Geometry and texture features, and a new SVM-based feature selection method. IEEE Systems Journal 2014;8(3):910–20.
[14] Mudigonda N, Rangayyan R, Desautels J. Gradient and texture analysis for the classification of mammographic masses. IEEE Trans Med Imaging 2000;19:1032–43.
[15] Mohanty AK, et al. Texture-based features for classification of mammograms using decision tree. Neural Comput Appl 2012;23(3–4):1011.
[16] Ioan B, Alexandru G. Directional features for automatic tumor classification of mammogram images. Biomed Signal Process Control 2011;6:370–8.
[17] Moayedi F, et al. Contourlet-based mammography mass classification using the SVM family. Comput Biol Med 2010;40(4):373–83.
[18] Nunes J, et al. Image analysis by bidimensional empirical mode decomposition. Image Vis Comput 2003;21(12):1019–26.
[19] Bajaj V, et al. "Computer-aided diagnosis of breast cancer using bi-dimensional empirical mode decomposition. Neural Computing and Applications," Neural Computing and *Applications*. 2017. p. 1–9.
[20] Suckling J, et al. The mammographic image analysis society digital mammogram databas. Amsterdam: *2nd International Workshop on Digital Mammography*; 1994.
[21] Heath M, et al. The digital database for screening mammography. *5th International Workshop on Digital Mammography*; 2000.
[22] Huang N, et al. The empirical mode decomposition and the Hilbert spectrum for non-linear and non-stationary time series analysis. Proc R Soc Lond A 1998;454:903–95.
[23] Wu Z, Huang N. Ensemble empirical mode decomposition: a noise-assisted data analysis method. Adv Adapt Data Anal 2009;1(1):1–41.
[24] Torres M, et al. A complete ensemble empirical mode decomposition with adaptive noise. IEEE International Conference on Acoustics, Speech and Signal Processing (ICASSP) 2011:4144–7.
[25] Pisano E, et al. Contrast limited adaptive histogram equalization image processing to improve the detection of simulated spiculations in dense mammograms. J Digit Imaging 1998;11(4):193–200.
[26] Gonzalez R, Woods R. "Image Enhancement," in *Digital Image Processing*, New Jersy. Prentice-Hall Inc.; 2008. p. 276.
[27] Haralick R, Shanmugam K, Dinstein I. Texture features for image classification. IEEE Trans SMC 1973;3(6):610–21.
[28] Cortes C, Vapnik V. Support vector networks. Mach Learn 1995;20:273–97.
[29] Lachenbruch PA. Discriminant Analysis. Newyork: Hafner Press; 1975.
[30] Krizhevsky A A, Sutskever I, Hinton GE. Imagenet classification with deep convolutional neural networks. In: Advances in neural information processing systems; 2012. p. 1097105.
[31] Zeiler MD, Fergus R. Visualizing and understanding convolutional networks. In: European conference on computer vision. Springer; 2014. p. 818–33.
[32] Szegedy C, Liu W, Jia Y, Sermanet P, Reed S, Anguelov D. Going deeper with convolutions. In: Proceedings of the IEEE conference on computer vision and pattern recognition; 2015. p. 1–9.
[33] Simonyan K, Zisserman A. Very deep convolutional networks for large-scale image recognition. 2014. p. 1409–556. arXiv preprint. arXivpp.
[34] He K, Zhang X, Ren S, Sun J. Deep residual learning for image recognition. In: Proceedings of the IEEE conference on computer vision and pattern recognition; 2016. p. 770–8.
[35] Zhang X, Zhang Y, Han EY, Jacobs N, Han Q, Wangl X. Whole mammogram image classification with convolutional neural networks. In: Bioinformatics and Biomedicine (BIBM) 2017 IEEE International Conference on. IEEE; 2017. p. 700–4.
[36] Dhungel N, Carneiro G, Bradley AP. The automated learning of deep features for breast mass classification from mammograms. In: International Conference on Medical Image Computing and Computer-Assisted Intervention. Springer; 2016. p. 106–14.
[37] Geras KJ, Wolfson S, Kim S, Moy L, Cho K. High-Resolution Breast Cancer Screening with Multi-View Deep Convolutional Neural Networks. 2017. arXiv preprint arXiv:170307047.
[38] Yi D, Sawyer RL, Cohn III D, Dunnmon J, Lam C, Xiao X, et al. Optimizing and Visualizing Deep Learning for Benign/Malignant Classification in Breast Tumors. 2017. arXiv preprint arXiv:170506362.